Published in final edited form as:
Matrix Biol. 2008 July ; 27(6): 561–572. doi:10.1016/j.matbio.2008.03.001.

Sparc (Osteonectin) functions in morphogenesis of the pharyngeal skeleton and inner ear

Josep Rotllant[1,*], **Dong Liu**[2], **Yin-Lin Yan**[2], **John H. Postlethwait**[2], **Monte Westerfield**[2], and **Shao-Jun Du**[1]

1*Center of Marine Biotechnology, University of Maryland Biotechnology Institute, Baltimore, MD 21202.*

2*Institute of Neuroscience, University of Oregon, Eugene, OR 97403 USA.*

Abstract

Sparc (Osteonectin), a matricellular glycoprotein expressed by many differentiated cells, is a major non-collagenous constituent of vertebrate bones. Recent studies indicate that Sparc expression appears early in development, although its function and regulation during embryogenesis are largely unknown. We cloned zebrafish *sparc* and investigated its role during development, using a morpholino antisense oligonucleotide-based knockdown approach. Consistent with its strong expression in the otic vesicle and developing pharyngeal cartilages, knockdown of Sparc function resulted in specific inner ear and cartilage defects that are highlighted by changes in gene expression, morphology and behavior. We rescued the knockdown phenotypes by co-injecting *sparc* mRNA, providing evidence that the knockdown phenotype is due specifically to impairment of Sparc function. A comparison of the phenotypes of Sparc knockdown and known zebrafish mutants with similar defects places Sparc downstream of *sox9* in the genetic network that regulates development of the pharyngeal skeleton and inner ear of vertebrates.

Keywords

cartilage; Col2a1a; Osteonectin; otic vesicle; Otx1; Sox9; Sparc

INTRODUCTION

Sparc (secreted protein, acidic and rich in cysteine), also known as Osteonectin or BM-40 (basement membrane tumor matrix component), is a secreted calcium-binding glycoprotein that belongs to the matricellular protein family (Yan and Sage, 1999). Rather than acting as structural components of the extracellular matrix, members of this family mediate cell-matrix interactions (Bornstein, 1995). Sparc is a multifunctional protein with a high affinity for cations and hydroxyapatite that provides support to extracellular matrix and mediates the activities of a wide range of growth factors (Brekken and Sage, 2000). Phenotypic abnormalities revealed by loss-of-function studies also support the interpretation that Sparc mainly functions in cell–matrix interactions (Gilmour et al., 1998, Delany et al., 2003, Bradshaw et al., 2002, Bradshaw et al., 2003, Brekken et al., 2003, Eckfeldt et al., 2005).

*Author for correspondence: Josep Rotllant, Instituto de Investigaciones Marinas, IIM, CSIC, Eduardo Cabello 6, 36208 Vigo, Pontevedra, Spain. Tel: +34 986 23 19 30; Fax: +34 986 29 27 62; E-Mail: rotllant@iim.csic.es.

Initially purified from bovine bone matrix (Termine et al., 1981), Sparc is also found in embryonic and adult tissues that undergo active proliferation and dynamic morphogenesis (Holland, 1987; Sage et al., 1989; Damjanovski et al., 1994; Yan and Sage, 1999; Damjanovski et al. 1998; Bradshaw & Sage, 2001; Padhi, 2004; Renn et al., 2006). With few exceptions, most animal species have a single Sparc-encoding gene (Laize et al., 2005). Sequence analysis reveals more than 70% amino acid identity among vertebrate Sparcs, whereas vertebrate and invertebrate Sparcs share only 38% identity (Yan & Sage, 1999; Laize et al., 2005). Surprisingly, no mutations in this gene have been identified in humans, although mouse *Sparc* mutants display various phenotypic abnormalities, such as cataracts, osteopenia, accelerated closure of dermal wounds, increased adiposity and enhanced growth of tumors (Gilmour et al., 1998, Delany et al., 2003, Bradshaw et al., 2002, Bradshaw et al., 2003, Brekken et al., 2003,). Knockout mice deficient for Sparc are normal when born, but develop severe eye pathology including cataracts, as well as tail defects and other bone-related defects after birth. The late onset of defects is likely due to severely reduced numbers of differentiated osteoblasts (Delany et al., 2003). However, studies carried out in other organisms suggest an important role for Sparc in early development. Inappropriate expression of Sparc in *Xenopus* embryos has dramatic affects on tissue morphogenesis (Damjanovski et al., 1997), whereas inactivation of Sparc in *C. elegans* by RNA interference suggests that Sparc is required for embryo viability (Fitzgerald and Schwarzbauer, 1998).

It has been hypothesized that the presence of other members of the SPARC family functionally compensate for the lack of SPARC expression (Brekken and Sage, 2001), leading to mild defects in SPARC-null mice. Therefore, in other organisms, such as C. elegans, where there is less redundancy, reduction in SPARC produces much more significant defects including embryonic lethality (Fitzgerald and Schwarzbauer, 1998)

Phylogenetic analyses of genome data indicate that gene duplication of SPARC gave rise to SPARCL1 (SPARC like-1), which in turn served as the common ancestral gene for the secretory calcium-binding phosphoprotein family (SCPPs), after the divergence of cartilaginous fish and bony fish but before the divergence of zfish and mammalian lineages. This implies that early vertebrate mineralization did not use SCPPs and that SPARC may be critical for initial mineralization in all bony fish (osteoichthyes). Consistent with this inference, no genes orthologous to mammalian enamel proteins, constituents of the secretory calcium-binding phosphoprotein (SCPP) family, have been identified in teleosts. Therefore, mammals apparently have more SPARC or SPARCL1 functional homologs than teleosts. Consequently, our observations in zebrafish likely uncover the significant roles of sparc.

Thus, the precise function of Sparc, especially during early embryogenesis, remains largely unknown. A recent report indicates that expression of the medaka *sparc* gene can serve as an early marker for skeletal and extracellular matrix (Renn et al, 2006). Its dynamic expression pattern during embryogenesis, similar to other vertebrates, suggests a conserved function of Sparc in vertebrates (Renn et al, 2006).

Here, we provide the first functional study of Sparc in zebrafish. We found that the zebrafish *sparc* gene is expressed in a temporally and spatially specific manner, with strong expression in the developing inner ear and pharyngeal cartilage. Knockdown of Sparc function by morpholino antisense oligonucleotides (MOs) produced a developmental phenotype that corresponds well to its expression pattern. We have further shown that Sparc interacts with genes in known genetic networks, unveiling its novel functions in regulating pharyngeal cartilage and inner ear development.

RESULTS

Conserved syntenies confirm that sparc is the zebrafish ortholog of human SPARC

Although sequences called *sparc* have been deposited in Genbank (Renn et al., 2006; Lien et al., 2006; Whitehead et al., 2005; Pahdi et al., 2004; Kawasaki et al., 2004), there has as yet been no analysis of conserved syntenies of the zebrafish *sparc* gene. *SPARC* is on the long arm of human chromosome 5 (Hsa5) (Fig. 1A), and immediately adjacent are *ATOX1*, *G3BP1*, and *GLRA1* (Fig. 1B). The best reciprocal blast hits (RBH) for two of these human genes lie as immediate neighbors of zebrafish *sparc* (Fig. 1C) on linkage group 14 (LG14)(Fig. 1D). Because RBH is a generally recognized method for the identification of likely orthologs (Wall et al., 2003), we conclude that these zebrafish genes are orthologs of *G3BP1* and *GLRA1* in the human genome. This evidence shows that, except for the loss of an ortholog of *ATOX1*, this region of the genome has been retained intact in gene order (*sparc—g3bp1—glra1*) for 450 million years since the divergence of the human and zebrafish lineages. The orthology of two genes adjacent to *sparc* and *SPARC* provides strong support for the orthology of *sparc* and *SPARC*, independent of phylogenetic trees (Laize et al., 2005).

Sparc is expressed dynamically in early zebrafish embryos

By RT-PCR, we detected *sparc* transcripts initially by 14 hours postfertilization (hpf), and expression subsequently increased and persisted (Fig. 2A). Whole-mount mRNA in situ hybridization showed that the otic placode was the initial site of strong expression in 14 hpf embryos (data not shown). By 24 hpf, *sparc* transcripts were present in the caudal fin fold, notochord, floor plate and somites, in addition to the otic vesicle (Fig.2B–D). At 72 hpf, *sparc* messenger RNA was still detectable in the otic vesicle, epidermal fin folds and floor plate but not in the notochord (Fig. 2E and data not shown), with additional expression in the pharyngeal skeleton, operculum, scapulocoracoid, endochondral disc, pectoral fin and pronephros (Fig. 2E–G and data not shown). Thus, zebrafish and medaka share a very similar expression pattern of *sparc* during embryogenesis (Renn et al., 2006). Similar results were also found in mouse, were sparc transcripts were detected in developing tissues, such as the otic vesicle (Mothe et al., 2001), notochord, somites and the embryonic skeleton (Holland et al., 1987;Mason et al., 1986)

Morpholino blockade of Sparc expression and splicing

To analyze the roles *sparc* plays in development, we took a loss-of-function approach: we designed antisense oligonucleotide morpholinos (MOs) to inhibit *sparc* translation and splicing (ATG-MO and E3I3-MO in Fig. 3A–B, respectively) in developing embryos. The specificity and efficacy of the morpholinos were analyzed either by their ability to inhibit protein translation in an in vitro transcription-translation assay (Fig. 3A) or their efficacy at inhibiting transcript processing in vivo as assayed by RT-PCR (Fig. 3C). The ATG-MO specifically blocked Sparc protein synthesis but had no effect on Smyd1a translation in the TNT assay. To demonstrate the efficacy of inhibition in vivo, we designed a splice-blocking morpholino targeted against the third coding exon-intron donor boundary (Figure 3B). When injected into zebrafish embryos, the splice-blocking morpholino resulted in the accumulation of a new transcript (401bp) due to the retention of the first 95 bp of intron 3 sequence as confirmed by sequencing the RT-PCR products of the *sparc* transcript from the knockdown embryos (Fig. 3C). This produced a transcript that is predicted to include a premature termination codon (33 amino acids after the splice site), thus encoding a peptide that lacks the highly conserved and likely essential C-terminal collagen and calcium binding domains (Laize et al., 2005). Quantitative analysis showed that 68% of the sparc transcripts were incorrectly spliced in embryos injected with 1 nl of 0.5 mM E3I3-MO, and injection of 1 nl of 1 mM E3I3-MO resulted in 100% improperly spliced transcripts (Figure 3C), compared with control MO injected or non-injected 48h embryos.

Thus, the specific inhibition of Sparc activity was MO dose dependent. By titrating the amount of MO injected, we determined the optimal MO doses that generated reproducible phenotypes without causing early lethality: 1nl of ATG-MO at a concentration of 0.5 mM, and 1 nl of E3I3-MO at a concentration of 1 mM. We injected these doses into 1- to 2-cell stage embryos, and examined development for 7 days. These embryos survived to 4 days postfertilisation (dpf), and about 20% were alive at 5 dpf, although none survived beyond 7 dpf. Most injected embryos developed normally until 30 hpf, when they appeared significantly smaller than the control MO injected or uninjected embryos. MO injected embryos were approximately 15% shorter in length and developed smaller and kinked pectoral fins (Fig. 4C–D). Among MO-injected animals, 81% (n=350) showed a severe reduction of their lower jaws (Fig. 4A–B), although dorsal components were relatively unaffected. Most MO injected animals (79%) displayed vestibular dysfunction, i.e., swimming or resting on their sides and circling only upon stimulation, consistent with a functional defect in the ear. The cartilage and inner ear phenotypes occur concurrently in almost all morpholino-injected animals (94%). Both morpholino strategies produced a similar phenotype in vivo, which was not observed in embryos injected with a scrambled control morpholino.

Sparc is required for pharyngeal cartilage morphogenesis

To analyze the lower jaw defects, we monitored cartilage patterning by Alcian blue staining (Fig. 4E–H). The cartilagenous neurocranium appeared relatively smaller but normally patterned after MO injection (Fig. 4F–H). In contrast, knockdown of Sparc resulted in absent or severely reduced Meckel's and ceratohyal cartilages (Fig. 4F–H), and the pharyngeal arches (ceratobranchials 1–5) failed to form (Fig. 4G–H). To learn whether Sparc knockdown affects the neural crest that is involved in cartilage patterning, we examined the expression of *dlx2a* in the subset of premigratory and post-migratory cranial neural crest cells that give rise to the pharyngeal arches (Akimenko, 1994, Miller at al., 2000). Expression of *dlx2a* was essentially normal after Sparc knockdown (Fig.3O–P). In contrast, *col2a1a* expression, which marks differentiating chondrocytes (Yan et al., 1995), was significantly reduced (Fig. 4I–J). This phenotype is similar to the phenotypes of *sox9* mutants we previously observed (Yan et al., 2005) where *col2a1a* expression is substantially reduced.

To understand the possible relationship of *col2a1a*, *sox9* and *sparc* expression, we analyzed expression of *sox9* genes in *sparc* knockdown embryos, and found that *sox9a* and *sox9b* expression domains were essentially normal (Fig.4K–N). Moreover, we found that *sparc* expression was substantially reduced or missing from the pharyngeal arches of *sox9a* (*jef*^{hi1134}), *sox9b* (*Df*^{b971}) and *jef*^{hi1134} (*Df*^{b971}) mutants (Fig. 5), suggesting that Sparc functions downstream of *sox9a* and upstream of *col2a1a* in the cascade of genes that regulate cartilage morphogenesis. However, it should be also noted that although *sox9a* and *sox9b* expression domains were patterned normally at 24 hpf after Sparc knockdown, their expression levels appeared somewhat reduced (Fig. 4K–N), suggesting that Sparc may provide positive feedback regulation of Sox9 expression.

Sparc is required for inner ear morphogenesis

Consistent with its strong and early expression in the otic placode, Sparc knockdown produced defects in the otic vesicle. To characterize these defects, we used known markers to monitor otic development (*dlx3b*, *eya1*, and *cldna*), specification (*stm* and *cldna*), and morphogenesis (*otx1, atp1a1a.4, msxc*). All markers except *otx1* showed normal expression in MO injected embryos at 24 hpf, suggesting that Sparc function is not required for otic induction or development through 24 hpf (Fig. 6A–H). However, *otx1* expression, which normally indicates the ventral epithelial region and developing posterior macula (Hammond et al., 2003), was absent or largely reduced in Sparc knockdown embryos (Fig. 6I–J). By 68 hpf, the ear was markedly smaller after Sparc knockdown, and the epithelial projections of the semicircular

canals, although present, failed to connect with each other to form the canals (Fig. 7A–B), and formation of the lateral and posterior semicircular canals was significantly disrupted. The otoliths however were present, consistent with the normal appearance of *starmaker* expression (Fig. 7A–B). Absence of *atp1a1a.4* expression further indicated the possible disruption of lateral and posterior semicircular canal formation (Fig. 7D). Examination of *msxc* expression, which normally marks the developing cristae, indicated failure of lateral crista development in MO-treated animals (Fig. 7E–F). The order of appearance of these elements excludes nonspecific developmental delay as the cause of the phenotype. FITC-phalloidin, which highlights actin-rich stereocilia of the ear sensory hair bundles, showed that in *sparc* MO-injected animals, the anterior and posterior maculae were closer to each other than in controls, presumably due to the loss of *otx1* expression between the two maculae (Fig. 7G–H).

sparc mRNA rescues defects caused by sparc MOs

To verify further the specificity of the defects produced by Sparc knockdown, we rescued ATG-MO and E3I3-MO injected embryos by co-injecting synthetic *sparc* mRNA with a modified ATG-MO binding site. Nearly complete rescue was achieved. The drastic reduction of differentiated cartilage after Sparc knockdown was rescued by co-injection of wild-type mRNA (Fig. 8A–H). The penetrance and severity of the phenotype was dose-dependent. We had better success rescuing the splice-blocking morpholino phenotypes; approximately 60% rescue in 1 mM E3I3-MO plus 750 μg/ml mRNA compared to 36 % with 0.5 mM ATG-MO plus 750 μg/ml mRNA (50 embryos). Similarly, the defects in ear differentiation, as indicated by various gene markers, were almost completely rescued by wild-type mRNA injection (Fig. 8L–T). *col2a1* expression in the notochord was also rescued (Fig. 8I–K), although the body shape was still somewhat abnormal.

These results demonstrate that exogenous wild-type *sparc* is sufficient to correct the defects in the otic vesicle and pharyngeal cartilage caused to *sparc* MOs, consistent with the interpretation that these developmental defects are due to reduced levels of Sparc protein function.

DISCUSSION

We examined the function of Sparc during development of zebrafish embryos and larvae. Previous studies of other teleosts (seabream and medaka) showed that *sparc* is dynamically expressed in skeletal and non-skeletal tissues from early development to adulthood, suggesting a potentially wide range of action (Estevao et al., 2005; Renn et al., 2006). The predicted zebrafish Sparc protein shares high similarity to the Sparc proteins of other vertebrates (Renn et al., 2006, Laize et al.,2005) and analysis of conserved syntenies provides independent evidence of orthology. Furthermore, the expression pattern of zebrafish *sparc* is comparable to medaka and sea bream (Renn et al., 2006; Redruello et al., 2005, Estevao et al., 2005). Based on previous studies that suggested Sparc may have numerous functions at late developmental stages, for instance, after birth in *Sparc* knock out mice (Yan et al., 1999), we anticipated a broad range of defects. Instead, we find that *sparc* functions mainly in the developing pharyngeal cartilage and inner ear, structures in which it is strongly expressed during early development.

We find that Sparc plays an important role in regulating pharyngeal cartilage development, but *dlx2* expression in *sparc* knockdown animals showed that *sparc* is not required for morphogenesis of the migratory and post-migratory cranial neural crest that contributes to the pharyngeal cartilage. We previously showed that *sox9* genes play a key role in chondrocyte morphogenesis (Yan et al., 2002, 2005). The defects in differentiated (Alcian blue positive) cranial cartilage observed in *sox9* mutants (Yan et al., 2005) are similar to those in *sparc* MO injected animals, suggesting that Sparc is directly involved in differentiation of cells within

pharyngeal precartilage condensations and that Sparc mediates at least some of the phenotypic defects of *sox9* mutants. The drastic reduction of *col2a1a* expression after *sparc* MO injection supports this interpretation. Because we also observed some reduction in the expression of both *sox9* genes in *sparc* MO injected animals, reduced *col2a1* expression after *sparc* MO injection could also indicate an indirect effect due to down regulation of *sox9* gene expression. Sox9 function is required for three morphogenetic processes in cartilage development: formation of orderly stacks of chondrocytes (Akiyama, et al., 2002, Yan et al., 2002), the individualization of cartilages (Kronenberg, 2003, Kawakami et al., 2006), and the shaping of specific skeletal elements (Yan et al., 2002). Whether these processes require a counter-adhesive effect on focal adhesions (Motamed and Sage, 1997), cell-matrix interactions that lead to additional cell recruitment, and/or Sparc-mediated signal transduction is still unclear.

The high mortality rate (100% by 7 dpf) of MO injected animals is presumably due to the defects in the pharyngeal arches; the animals can not feed and blood circulation through the aortic arches is impaired. Thus, the effect of Sparc knockdown on later development, such as the mineralization process, could not be determined.

In this study, we also demonstrated that Sparc knockdown produces a prominent and highly specific defect in inner ear development, failure to form the horizontal semicircular canal and lateral crista, and abnormal fusion of anterior and posterior maculae. The inner ear develops from the otic placode, a specialized ectodermal thickening that later forms the membranous labyrinth of the inner ear through a process of epithelial growth and remodeling (Haddon et al., 1991; Barald and Kelley, 2004). We can rule out a role of Sparc in early ear induction and patterning, because the ear vesicle forms normally and the majority of known ear markers (Liu et al., 2003) exhibit essentially normal expression after Sparc knockdown. The later ear defects due to Sparc knockdown thus indicate a role in differentiation of subparts of the ear. These defects are very similar to the ear defects of Otx1 knockdown animals (Hammond and Whitfield, 2006), and Sparc knockdown disrupt *otx1* expression in the ear. Hammond and Whitfield (2006) recently pointed out that because *otx1* is expressed in the zebrafish ear but not lamprey ear, Otx1 expression may reflect an evolutionary gain of the third semicircular canal and crista, and a subdivision of the single macula during evolution from agnathan to gnathostome vertebrates. The ear defects due to Sparc knockdown thus reveal an important yet unique developmental role of Sparc in the more recently evolved auditory sensory organ.

Because Otx1 is also expressed in pharyngeal arches and skeletal elements (Thisse et al., 2004), it is possible that pharyngeal defects in *sparc* MO injected animals are partially due to a loss of *otx1* expression and partially due to feedback regulation of *sox9* genes by Sparc. These inferences raise a puzzling question of how a matricellular protein can regulate expression of transcription factor genes, in this case *otx1* and *sox9*. The role of Sparc in cell-matrix interactions may hold the answer; Sparc may mediate or trigger signal transduction pathways required for activation or maintenance of target gene transcription. This notion could be explored by identifying extracellular signaling molecules that act upstream of the genes encoding Sox9, Otx1 and Sparc. We recently learned that Fgfs are regulators of *sox9* gene expression in the ear (Hans et al., 2007 and unpublished observations), and an earlier report indicates that mutations in *fgf20a* down regulate *sparc* expression and block the initiation of fin regeneration (Whitehead et al., 2005). Thus, members of the Fgf family of signaling molecules may be good candidates for signaling molecules that interact with Sparc.

EXPERIMENTAL PROCEDURES

Experimental animals

Zebrafish embryos were cultured as previously described (Westerfield, 2007) and staged by standard criteria (Kimmel et al., 1995) or by hours (hpf) or days (dpf) postfertilization.

Experiments were performed using the AB wild-type strain (Zebrafish International Resource Center) and *sox9a* (*jef*^{hi1134}) and *sox9b* (*Df(LG03:sox8,sox9b)*^{b971}) mutants (Yan et al., 2005). To inhibit embryo pigmentation, embryo medium was supplemented with 0.003% (w/v) 2-phenylthiourea (Westerfield, 2007). For histology, dechorionated embryos were fixed overnight at 4°C in 4% paraformaldehyde in 1x PBS, washed in PBS, and either stored at 4° C in 1x PBS for FITC-phalloidin and cartilage staining, or dehydrated through a methanol series and stored at −20°C in 100% methanol for in situ hybridization.

RNA isolation & RT-PCR

The full length transcript of zebrafish *sparc* was obtained by RT-PCR (GenBank Accession Number: BC071436). Total RNA was extracted from zebrafish embryos at 0, 3, 6, 9, 12, 14 and 19 hpf and 1, 2, 3, 4, 5 and 6 dpf using TRIzol (Invitrogen). First-strand cDNA was synthesized according to the Life Science Inc. protocol using AMV reverse transcriptase. The PCR reaction mixtures were prepared using the PCR Master Mix (Promega) and PCR was performed for 35 cycles under standard conditions at 58°C annealing temperature. Temporal expression profiles of *sparc* were determined by RT-PCR using the primers (5'primer/3'primer), TGCTTAGGCTGAAACTCAAGATGAG / GCATCAATGGAAGACGTCCTTAGAT. PCR was also carried out to amplify *ef1a* cDNA as a positive control.

Morpholino knockdown

Morpholino antisense oligonucleotides (MOs) were synthesized by GeneTools (Corvallis, OR). Two independent MOs, a translation blocker (ATG-MO: 5'GATCCAAACCCTCATCTTGAGTTTC3') and a splicing blocker (E3I3-MO: 5'GAAAAATGAACTCACTCTCAGCAAT3'), were used to target *sparc*. A scrambled MO with no known target in zebrafish, *c*MO, 5'-CCTCTTACCTCAGTTACAATTTATA-3' was used as control. The MOs were resuspended in 1x Danieau buffer (58 mM NaCl, 0.7 mM KCl, 0.4 mM $MgSO_4$, 0.6 mM $Ca(NO_3)_2$, 5 mM HEPES, pH 7.6) to a final concentration of 0.5 mM or 1 mM. Approximately, 1 nl was injected into one- or two-cell stage embryos. Eckfeldt et al (2005) used an ATG-MO against *sparc* in a hematopoietic defect study but did not report any cartilage and inner ear defects. The first 12 bases of their MO are identical to the last 12 bases of our independently designed ATG-MO.

Morpholino specificity

The efficacy of the MOs to block translation or splicing of *sparc* specifically was analyzed using either an in vitro translation assay or RT-PCR.

Function of the ATG-MO was assessed in an in vitro transcription and translation-coupled system (TNT Coupled Reticulocyte Lysate Systems; Promega). The amplified full length *sparc* cDNA was subcloned into the pCS2+ vector. The pCS2+ vector utilizes the SP6 RNA polymerase binding site that can be used directly for *in vitro* transcription-translation assays. The assay was performed according to the instructions provided with the Promega TNT Coupled Reticulocyte Lysate Systems using [alpha][^{35}S] methionine. The synthesized proteins were analyzed by SDS gel electrophoresis on a 10% acrylamide gel and visualized by autoradiography after 2 hour exposure at room temperature. pCS2^{+}−*smyd1a* (Tan et al., 2006) was used as a control for this assay.

To test for disruption of splicing, RT-PCR was performed (primers: exon 1 forward, 5'GCTGAAACTCAAGATGAG-3'; exon 4 reverse, 5'TCCAATCGGAGACTTCGAGCA-3'). Total RNA from 15 uninjected 48hpf embryos, 15 embryos injected with 1nl of 1 mM cMO, 15 embryos injected with 1 nL of 0.5 mM E3I3-MO

and 15 embryos injected with 1 nL of and 1 mM E3I3-MO were collected, the cDNA transcribed following the above protocol.

Whole-mount in Situ Hybridization

Whole-mount in situ hybridization was performed using digoxigenin-labeled antisense probes as previously described (Du et al., 2001). Antisense riboprobes were made from linearized full length *Danio rerio sparc* cDNA (GenBank Accession number: BC071436) (primers: forward 5'TGCTTAGGCTGAAACTCAAGATGAG3'; reverse 5'GCATCAATGGAAGACGTCCTTAGAT3') and the partial Danio rerio Col2a1 cDNA (GenBank Accession number U23822) (primers: forward 5'CAGAGGATTCACTGGTCTGCAGGG3'; reverse: 5' TCCACTCCGAACTCCTGATCTGCTC3'). Other antisense RNA probes used in this study were *sox9a* and *sox9b* (Chiang et al., 2001), *dlx2a* (Akimenko et al., 1994), *otx1* (Whitfield, 1996), *stm* (Sollner et al., 2003), *dlx3b* (Ekker et al., 1992), *cldna* (Kollmar et al., 2001), *eya1* (Hammond, 2003), *msxc* (Ekker et al., 1992) and *atp1a1a.4* (Blasiole, 2003).

mRNA-rescue

To generate the capped mRNA, zebrafish *sparc* cDNA (GenBank Accession number: BC071436) was subcloned into pCS2+ plasmids. Capped mRNA was transcribed *in vitro* using the SP6 Message Machine Kit (Ambion). The $PCS2^{+}$-*sparc* construct used in the rescue experiments includes a Kozak sequence upstream of the ATG, instead of the endogenous zebrafish sequence, resulting in five mismatches between the antisense sequences and the rescue mRNA. Thus, the capped mRNA rescue constructs were not susceptible to the MOs. Furthermore, becuase the *sparc* mRNA does not contain the intron sequences targeted by the splicing morpholino, the same *sparc* mRNA can be used, in combination with the translation or splice-blocking morpholinos, for the RNA rescue experiment. mRNA was injected into 1- to 2-cell stage embryos either alone or in the presence of a MO. For each rescue experiment, the amount of mRNA injected was titrated for the maximal doses that could be injected. For rescue experiments, approximately 1 nl of 0.5 mM (4μg/μl) ATG-MO or 1 mM (8μg/μl) E3I3-MO was injected together with 1 nl two different mRNA concentrations (325 μg/ml and 750 μg/ml) per embryo. Approximately 200 embryos were used. Around 50 embryos were co-injected with each MO (and the two different sparc RNA concentrations).

FITC-phalloidin staining

Whole-mount embryos were stained for actin with FITC-phalloidin as described previously (Haddon and Lewis, 1996), mounted in Vectashield (Vector Laboratories) and imaged with a BioRad confocal microscope.

Cartilage staining

Alcian blue was used for cartilage staining in fixed embryos as described (Kimmel et al., 1998; Miller et al., 2000). Briefly, fixed embryos were rinsed with 100 mM Tris pH7.5/10 mM $MgCl_2$ and stained overnight with 0.04% alcian blue, 80% ethanol, 100 mM Tris pH7.5, 10 mM $MgCl_2$. After a series of washes with 80%, 50% and 25% ethanol/Tris each for 10 min, embryos were treated with 0.5% KOH, 3% H_2O_2 for 20 min. Stained embryos were preserved and observed in 50% glycerol, 0.1% KOH solution.

ACKNOWLEDGEMENT

We would like to thank Tanya Whitfield, Brain Blasiole and David Stock for generously sharing probes. This research was carried out with the financial support of The European Commission Marie Curie Outgoing International Fellowship (MOIF-CT-2005007782) and Ramon Y Cajal (MEC-CSIC) contract to JR and by the National Institutes of Health DC04186, GM58537, RR10715, and HD22486.

REFERENCES

Akimenko MA, Ekker M, Wegner J, Lin W, Westerfield M. Combinatorial expression of three zebrafish genes related to distal-less: part of a homeobox gene code for the head. J. Neurosci 1994;14(6):3475–3486. [PubMed: 7911517]

Akiyama H, Chaboissier MC, Martin JF, Schedl A, de Crombrugghe B. The transcription factor Sox9 has essential roles in successive steps of the chondrocyte differentiation pathway and is required for expression of Sox5 and Sox6. Genes Dev 2002 Nov 1;16(21):2813–2828. [PubMed: 12414734]

Barald KF, Kelley MW. From placode to polarization: new tunes in inner ear development. Development 2004;131(17):4119–4130. [PubMed: 15319325]

Blasiole B, Degrave A, Canfield V, Boehmler W, Thisse C, Thisse B, Mohideen MA, Levenson R. Differential expression of Na,K-ATPase alpha and beta subunit genes in the developing zebrafish inner ear. Dev Dyn 2003 Nov;228(3):386–92. [PubMed: 14579377]

Bornstein P. Diversity of function is inherent in matricellular proteins: an appraisal of thrombospondin 1. J Cell Biol 1995;130(3):503–506. [PubMed: 7542656]

Bradshaw AD, Graves DC, Motamed K, Sage EH. SPARC-null mice exhibit increased adiposity without significant differences in overall body weight. Proc. Natl. Acad. Sci. USA 2003;100(10):6045–6050. [PubMed: 12721366]

Bradshaw AD, Reed MJ, Sage EH. SPARC-null mice exhibit accelerated cutaneous wound closure. J. Histochem. Cytochem 2002;50(1):1–10. [PubMed: 11748289]

Bradshaw AD, Sage EH. SPARC, a matricellular protein that functions in cellular differentiation and tissue response to injury. J. Clin. Invest 2001;107(9):1049–1054. [PubMed: 11342565]

Brekken RA, Puolakkainen P, Graves DC, Workman G, Lubkin SR, Sage EH. Enhanced growth of tumors in SPARC null mice is associated with changes in the ECM. J. Clin. Invest 2003 Feb;111(4):487–495. [PubMed: 12588887]

Brekken RA, Sage EH. SPARC, a matricellular protein: at the crossroads of cell-matrix communication. Matrix Biol 2001;19(8):816–827. [PubMed: 11223341]

Chiang EF, Pai CI, Wyatt M, Yan YL, Postlethwait J, Chung B. Two sox9 genes on duplicated zebrafish chromosomes: expression of similar transcription activators in distinct sites. Dev. Biol 2001;231(1):149–163. [PubMed: 11180959]

Damjanovski S, Huynh MH, Motamed K, Sage EH, Ringuette EH. Regulation of SPARC expression during early Xenopus development: evolutionary divergence and conservation of DNA regulatory elements between amphibians and mammals. Dev. Genes Evol 1998;207(7):453–461. [PubMed: 9510540]

Damjanovski S, Malaval L, Ringuette MJ. Transient expression of SPARC in the dorsal axis of early Xenopus embryos: correlation with calcium-dependent adhesion and electrical coupling. Int. J. Dev. Biol 1994;38(3):439–446. [PubMed: 7848827]

Delany AM, Kalajzic I, Bradshaw AD, Sage EH, Canalis E. Osteonectin-null mutation compromises osteoblast formation, maturation, and survival. Endocrinology 2003;144(6):2588–2596. [PubMed: 12746322]

Du SJ, Frenkel V, Kindschi G, Zohar Y. Visualizing normal and defective bone development in zebrafish embryos using the fluorescent chromophore calcein. Dev. Biol 2001;238(2):239–246. [PubMed: 11784007]

Eckfeldt CE, Mendenhall EM, Flynn CM, Wang TF, Pickart MA, Grindle SM, Ekker SC, Verfaillie CM. Functional analysis of human hematopoietic stem cell gene expression using zebrafish. PLoS Biol 2005;3(8):e254. [PubMed: 16089502]

Ekker M, Akimenko MA, Bremiller R, Westerfield M. Regional expression of three homeobox transcripts in the inner ear of zebrafish embryos. Neuron 1992;9(1):27–35. [PubMed: 1352984]

Estevao MD, Redruello B, Canario AV, Power DM. Ontogeny of osteonectin expression in embryos and larvae of sea bream (Sparus auratus). Gen. Comp. Endocrinol 2005;142(1–2):155–162. [PubMed: 15862559]

Fitzgerald M, Schwarzbauer JE. Importance of the basal lamina protein SPARC for viability and fertility in Caenorhabditis elegans. Curr Biol 1998;8:1285–1288. [PubMed: 9822581]

Gilmour DT, Lyon GJ, Carlton MB, Sanes JR, Cunningham JM, Anderson JR, Hogan BL, Evans MJ, Colledge WH. Mice deficient for the secreted glycoprotein Mice deficient for the secreted glycoprotein SPARC/osteonectin/BM40 develop normally but show severe age-onset cataract formation and disruption of the lens. EMBO J 1998;17(7):1860–1870. [PubMed: 9524110]

Haddon CM, Lewis JH. Hyaluronan as a propellant for epithelial movement: the development of semicircular canals in the inner ear of Xenopus. Development 1991;112(2):541–550. [PubMed: 1794322]

Haddon C, Lewis J. Early ear development in the embryo of the zebrafish, Danio rerio. J. Comp. Neurol 1996;365(1):113–128. [PubMed: 8821445]

Hammond KL, Loynes HE, Folarin AA, Smith J, Whitfield TT. Hedgehog signalling is required for correct anteroposterior patterning of the zebrafish otic vesicle. Development 2003;130(7):1403–1417. [PubMed: 12588855]

Hammond KL, Whitfield TT. The developing lamprey ear closely resembles the zebrafish otic vesicle: otx1 expression can account for all major patterning differences. Development 2006;133(7):1347–1357. [PubMed: 16510503]

Hans S, Christison J, Liu D, Westerfield M. Fgf-dependent otic induction requires competence provided by Foxi1 and Dlx3b. BMC Dev Biol 2007;19(7):5. [PubMed: 17239227]

Holland PW, Harper SJ, McVey JH, Hogan BL. In vivo expression of mRNA for the Ca++-binding protein SPARC (osteonectin) revealed by in situ hybridization. J. Cell Biol 1987;105(1):473–482. [PubMed: 2440898]

Kawakami Y, Rodriguez-Leon J, Izpisua Belmonte JC. The role of TGFbs and Sox9 during limb chondrogenesis. Current Opinion in Cell Biology 2006 2006;18:723–729.

Kawasaki K, Suzuki T, Weiss KM. Genetic basis for the evolution of vertebrate mineralized tissue. Proc. Natl. Acad. Sci. U.S.A 2004;101(31):11356–11361. [PubMed: 15272073]

Kimmel CB, Ballard WW, Kimmel SR, Ullmann B, Schilling TF. Stages of embryonic development of the zebrafish. Dev Dyn 1995;203(3):253–310. [PubMed: 8589427]

Kimmel CB, Miller CT, Kruze G, Ullmann B, BreMiller RA, Larison KD, Snyder HC. The shaping of pharyngeal cartilages during early development of the zebrafish. Dev. Biol 1998;203(2):245–263. [PubMed: 9808777]

Kollmar R, Nakamura SK, Kappler JA, Hudspeth AJ. Expression and phylogeny of claudins in vertebrate primordia. Proc. Natl. Acad. Sci. U S A 2001;98(18):10196–10201. [PubMed: 11517306]

Kronenberg HM. Developmental regulation of the growth plate. Nature 15 2003;423(6937):332–336.

Laize V, Pombinho AR, Cancela ML. Characterization of Sparus aurata osteonectin cDNA and in silico analysis of protein conserved features: evidence for more than one osteonectin in Salmonidae. Biochimie 2005;87(5):411–420. [PubMed: 15820747]

Lien CL, Schebesta M, Makino S, Weber GJ, Keating MT. Gene expression analysis of zebrafish heart regeneration. PLoS Biol 2006;4(8):E260. [PubMed: 16869712]

Liu D, Chu H, Maves L, Yan YL, Morcos PA, Postlethwait JH, Westerfield M. Fgf3 and Fgf8 dependent and independent transcription factors are required for otic placode specification. Development 2003;130(10):2213–2224. [PubMed: 12668634]

Miller CT, Schilling TF, Lee K, Parker J, Kimmel CB. Sucker encodes a zebrafish Endothelin-1 required for ventral pharyngeal arch development. Development 2000;127(17):3815–3828. [PubMed: 10934026]

Mason IJ, Murphy D, Munke M, Francke U, Elliott RW, Hogan BL. Developmental and transformation-sensitive expression of the Sparc gene on mouse chromosome 11. Embo J 1986;5(8):1831–1837. [PubMed: 3758028]

Motamed K, Sage EH. Regulation of vascular morphogenesis by the matricellular protein SPARC. Kidney Int 1997;51(5):1383–1387. [PubMed: 9150448]

Padhi BK, Joly L, Tellis P, Smith A, Nanjappa P, Chevrette M, Ekker M, Akimenko MA. Screen for genes differentially expressed during regeneration of the zebrafish caudal fin. Dev. Dyn 2004;231 (3):527–541. [PubMed: 15376328]

Redruello B, Estevao MD, Rotllant J, Guerreiro PM, Anjos LI, Canario AV, Power DM. Isolation and characterization of piscine osteonectin and downregulation of its expression by PTH-related protein. J. Bone Miner. Res 2005;20(4):682–692. [PubMed: 15765188]

Renn J, Schaedel M, Volff JN, Goerlich R, Schartl M, Winkler C. Dynamic expression of sparc precedes formation of skeletal elements in the Medaka (Oryzias latipes). Gene 2006;372:208–218. [PubMed: 16545530]

Renn J, Winkler C, Schartl M, Fischer R, Goerlich R. Zebrafish and medaka as models for bone research including implications regarding space-related issues. Protoplasma 2006;229(2–4):209–214. [PubMed: 17180503]

Sage H, Vernon RB, Decker J, Funk S, Iruela-Arispe ML. Distribution of the calcium-binding protein SPARC in tissues of embryonic and adult mice. J. Histochem. Cytochem 1989;37(6):819–829. [PubMed: 2723400]

Sollner C, Burghammer M, Busch-Nentwich E, Berger J, Schwarz H, Riekel C, Nicolson T. Control of crystal size and lattice formation by starmaker in otolith biomineralization. Science 10 2003;302 (5643):282–286.

Tan X, Rotllant J, Li H, De Deyne P, Du SJ. SmyD1, a histone methyltransferase, is required for myofibril organization and muscle contraction in zebrafish embryos. Proc. Natl. Acad. Sci. USA 2006;103(8): 2713–2718. [PubMed: 16477022]

Termine JD, Kleinman HK, Whitson SW, Conn KM, McGarvey ML, Martin GR. Osteonectin, a bone-specific protein linking mineral to collagen. Cell 1981;1:99–105. [PubMed: 7034958]

Thisse B, Heyer V, Lux A, Alunni A, Degrave A, Seiliez I, Kirchner J, Parkhill J-P, Thisse C. Spatial and Temporal Expression of the Zebrafish Genome by Large-Scale In Situ Hybridization Screening. Meth. Cell. Biol 2004;77:505–519.

Wall DP, Fraser HB, Hirsh AE. Detecting putative orthologs. Bioinformatics 2003;19:1710–1711. [PubMed: 15593400]

Westerfield, M. The Zebrafish Book: A guide for the laboratory use of Zebrafish (Danio rerio). Vol. 5th Edition. Eugene: Univ. of Oregon Press; 2007.

Whitehead GG, Makino S, Lien CL, Keating MT. Fgf20 is essential for initiating zebrafish fin regeneration. Science 23 2005;310(5756):1957–1960.

Whitfield TT, Granato M, van Eeden FJ, Schach U, Brand M, Furutani-Seiki M, Haffter P, Hammerschmidt M, Heisenberg CP, Jiang YJ, Kane DA, Kelsh RN, Mullins MC, Odenthal J, Nusslein-Volhard C. Mutations affecting development of the zebrafish inner ear and lateral line. Development 1996;123:241–254. [PubMed: 9007244]

Yan Q, Sage EH. SPARC, a matricellular glycoprotein with important biological functions. J. Histochem. Cytochem 1999;47(12):1495–1506. [PubMed: 10567433]

Yan YL, Hatta K, Riggleman B, Postlethwait JH. Expression of a type II collagen gene in the zebrafish embryonic axis. Dev. Dyn 1995;203(3):363–376. [PubMed: 8589433]

Yan YL, Miller CT, Nissen RM, Singer A, Liu D, Kirn A, Draper B, Willoughby J, Morcos PA, Amsterdam A, Chung BC, Westerfield M, Haffter P, Hopkins N, Kimmel C, Postlethwait JH. A zebrafish sox9 gene required for cartilage morphogenesis. Development 2002;29(21):5065–5079. [PubMed: 12397114]

Yan YL, Willoughby J, Liu D, Crump JG, Wilson C, Miller CT, Singer A, Kimmel C, Westerfield M, Postlethwait JH. A pair of Sox: distinct and overlapping functions of zebrafish sox9 co-orthologs in craniofacial and pectoral fin development. Development 2005;132(5):1069–1083. [PubMed: 15689370]

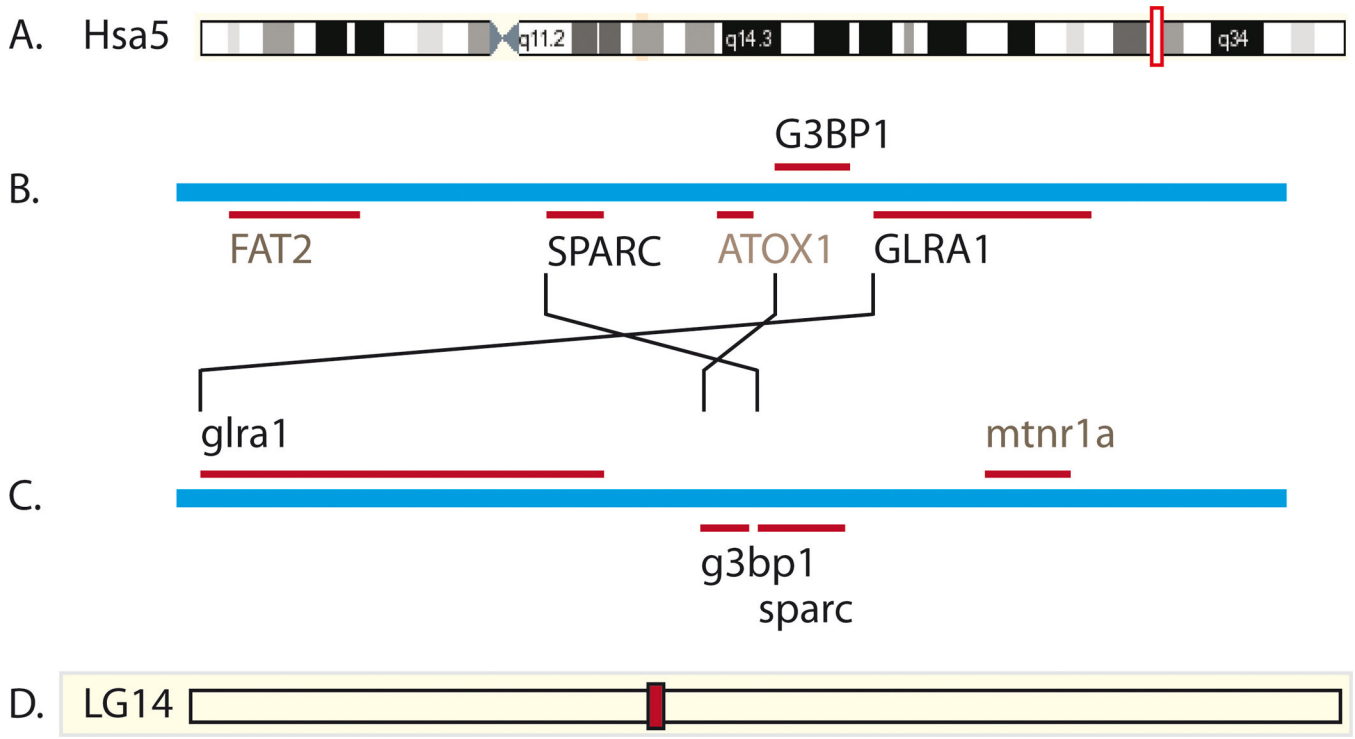

Figure 1. Conserved syntenies confirm the orthology of zebrafish *sparc* and human *SPARC* genes

(A) human chromosome 5 (Hsa5), with the location of *SPARC* boxed in red and expanded in (B). (C) the *sparc* containing region of the zebrafish genome, which resides in linkage group (LG) 14, in the red boxed region (D). In both species, *sparc* or *SPARC* and two of the three closest neighbors on one side are arranged in the same order, thus demonstrating conservation of this chromosome segment in both lineages from the last common ancestor of zebrafish and humans. The human *ATOX1* gene does not appear to have an ortholog in the zebrafish genome (Zv7).

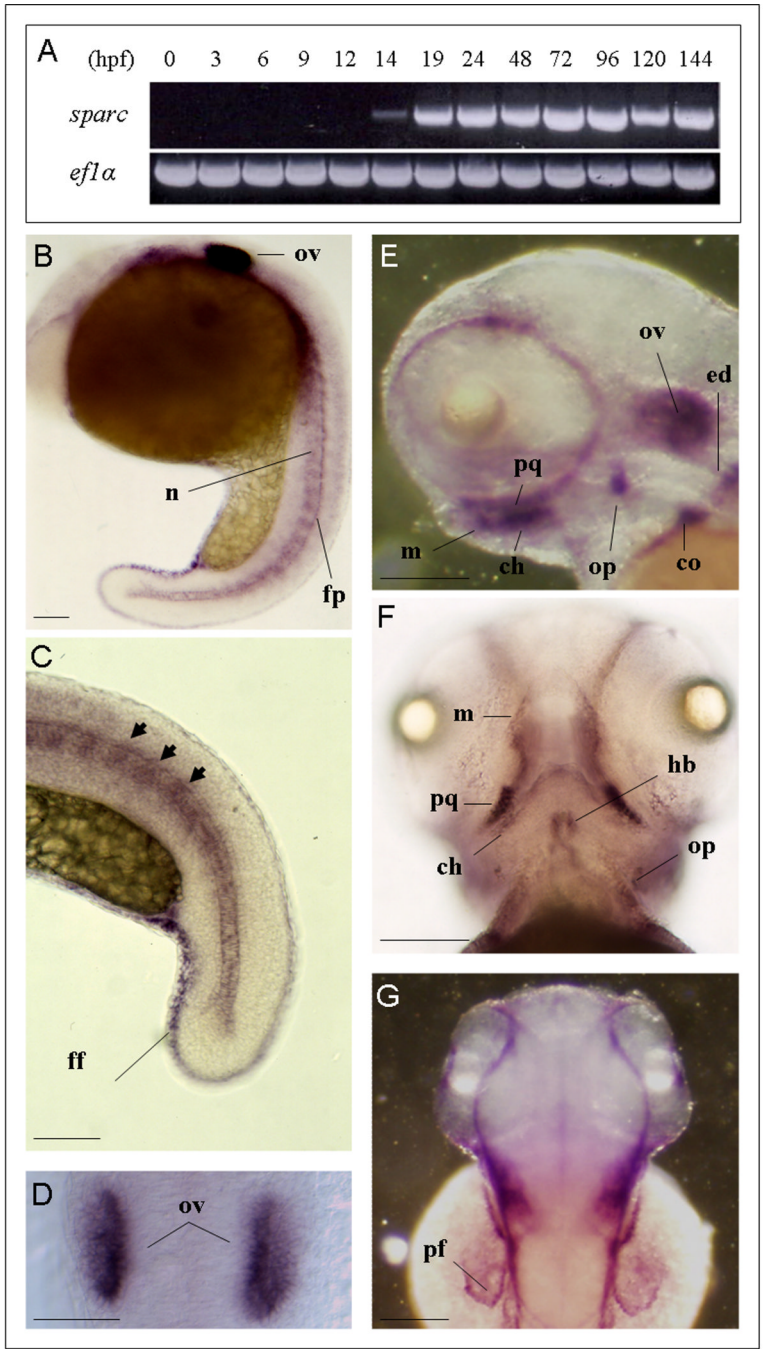

Figure 2. The *sparc* gene is dynamically expressed during early development

(A) RT-PCR analyses of the temporal expression pattern of *sparc*. (B–G) In situ hybridization showing the expression pattern of *sparc*. (C) Periodic expression of *sparc* expression in the notochord (arrows). (B, C, D) 24 hpf embryos. (E, F, G) lateral (E), ventral (F) and dorsal (G) views of the head at 72 hpf. ov (otic vesicle), n (notochord), fp (floor plate), m (Meckel's cartilage), op (opercle), ch (ceratohyal), co (scapulocoracoid), ed (endochondral disc), ff (fin fold), pf (pectoral fin), pq (palatoquadrate), hb (hypobranchial). (B,C,E) anterior to the left, dorsal to the top; (D,F,G) dorsal to the top. Scale bars: 100 μm.

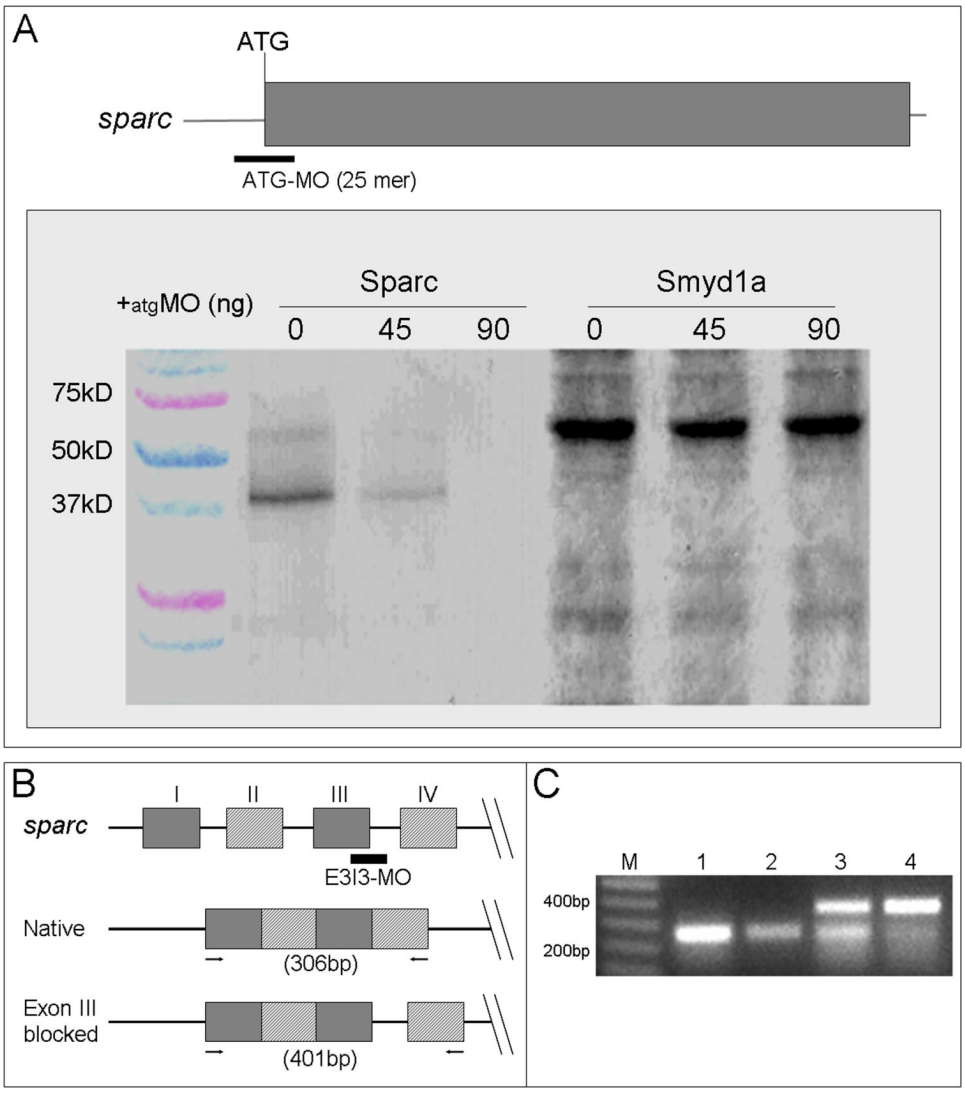

Figure 3. ATG and splice blocking morpholinos (MO) knock down Sparc expression

(A) ATG-MO specifically blocks the expression of Sparc protein in an *in vitro* transcription and translation assay (TNT) but has no effect on translation of a control, Smyd1a. (B) Location of the splice blocker E3I3-MO at the exon 3/intron 3 junction. (C) E3I3-MO blocks the splicing of *sparc* transcript. RT-PCR shows the defective splicing induced by the E3I3-MO. Compared with the PCR results from non-injected and control (cMO) injected embryos where a single band (306 bp) is generated (lane 1 and 2), two bands (306 bp and 401 bp) are detected in the 0.5 mM (lane 3) and 1 band in the 1 mM (lane 4) E3I3-MO-injected 48 hpf embryos. In lane 4, the 401 bp band, which is the major PCR product, is a result of defective splicing due to use of a cryptic splice donor located 95 bp 3' of the normal exon 3/intron 3 splice site in intron 3 as shown by DNA sequencing (data not shown).

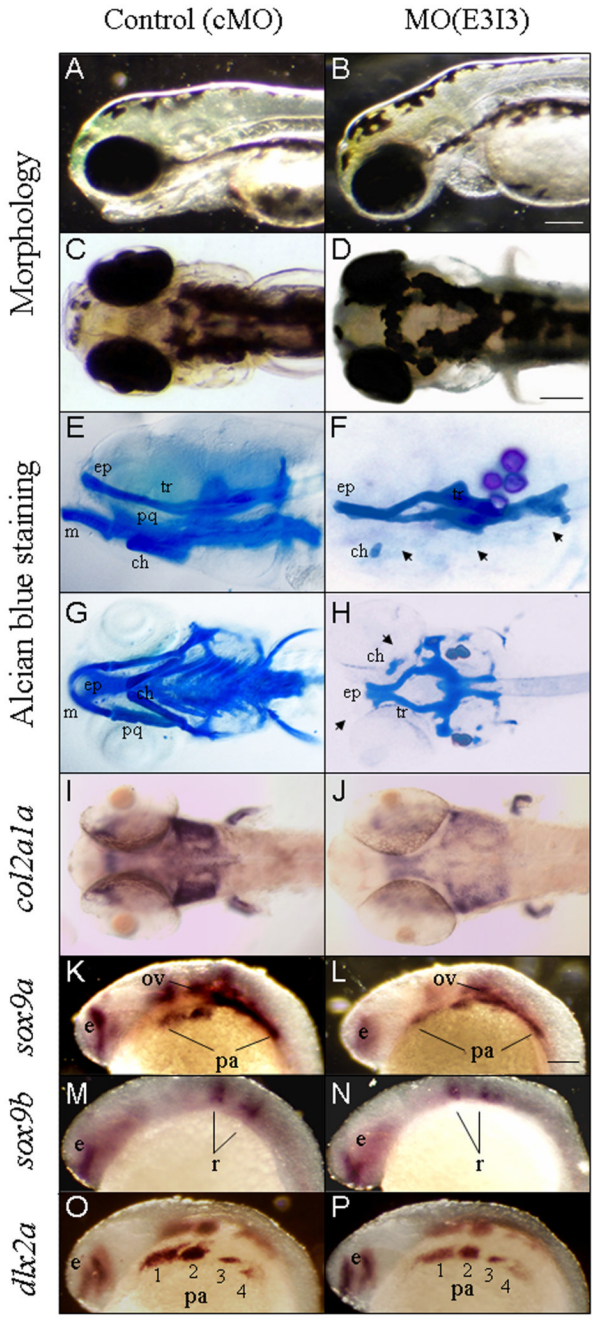

Figure 4. Knockdown of Sparc affects cartilage and ear development

(A–D) Morphology of the control (A, lateral view, and C, dorsal view) and *sparc* MO injected (B, lateral view, and D, dorsal view) embryos at 96 hpf. Note the reduced lower jaw in the MO injected embryos (B). (E–H) Alcian blue staining of the control (E, lateral view, and G, ventral view) and sparc MO injected (F, lateral view, and H, ventral view) embryos. Note the lack of differentiated pharyngeal arches in the MO injected embryos (F and H). The cartilage in the ethmoid plate (ep) and the trabecula (tr) is relatively unaffected in the MO injected embryo (I–J) Whole-mount mRNA in situ hybridization analysis of *col2a1* expression in 72 hpf embryos. In *sparc* MO injected embryos (ventral views), *col2a1* expression is strongly reduced, although not completely absent (J). (K–N) Whole-mount mRNA in situ hybridization analysis of

sox9a and *sox9b* expression in 24 hpf embryos. (O–P) Whole-mount mRNA in situ hybridization analysis of *dlx2a* expression in 24 hpf embryos. By this stage, embryos have formed four pairs of pharyngeal arches, the mandibular (1), hyoid (2), and the first (3) and second (4) pharyngeal arches. Abbreviations: m, Meckel's cartilage; e, eye; ep, ethmoid plate; ch, ceratohyal; ov, otic vesicle; pa, pharyngeal arches; pq, palatoquadrate; r, rhombomeres; tr, trabecula. (A–P) anterior to the left; (A–B, E–F, K–P) dorsal to the top; Scale bars: (A–B) 100 μm; (C–J) 100 μm; (K–P) 100 μm.

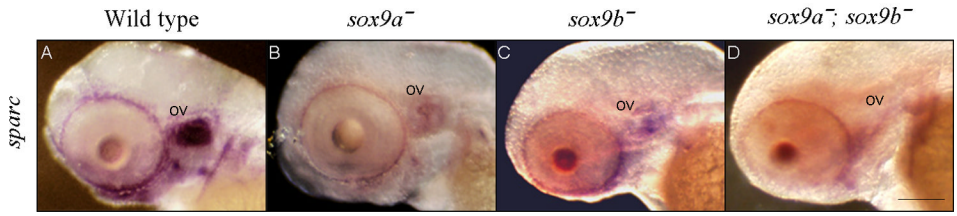

Figure 5. Sox9a and Sox9b are required for normal *sparc* gene expression

(M–P) lateral views of *sparc* expression in 72 hpf larval heads, showing decreased expression in *sox9* mutants. (A) Wild type; (B) *sox9a*$^{-}$ mutant; (C) *sox9b*$^{-}$ mutant; (D) *sox9a*$^{-}$;*sox9b*$^{-}$ double mutant. Abbreviations: ov, otic vesicle; (A–D) anterior to the left and dorsal to the top. Scale bars: in (A–D) 100 μm.

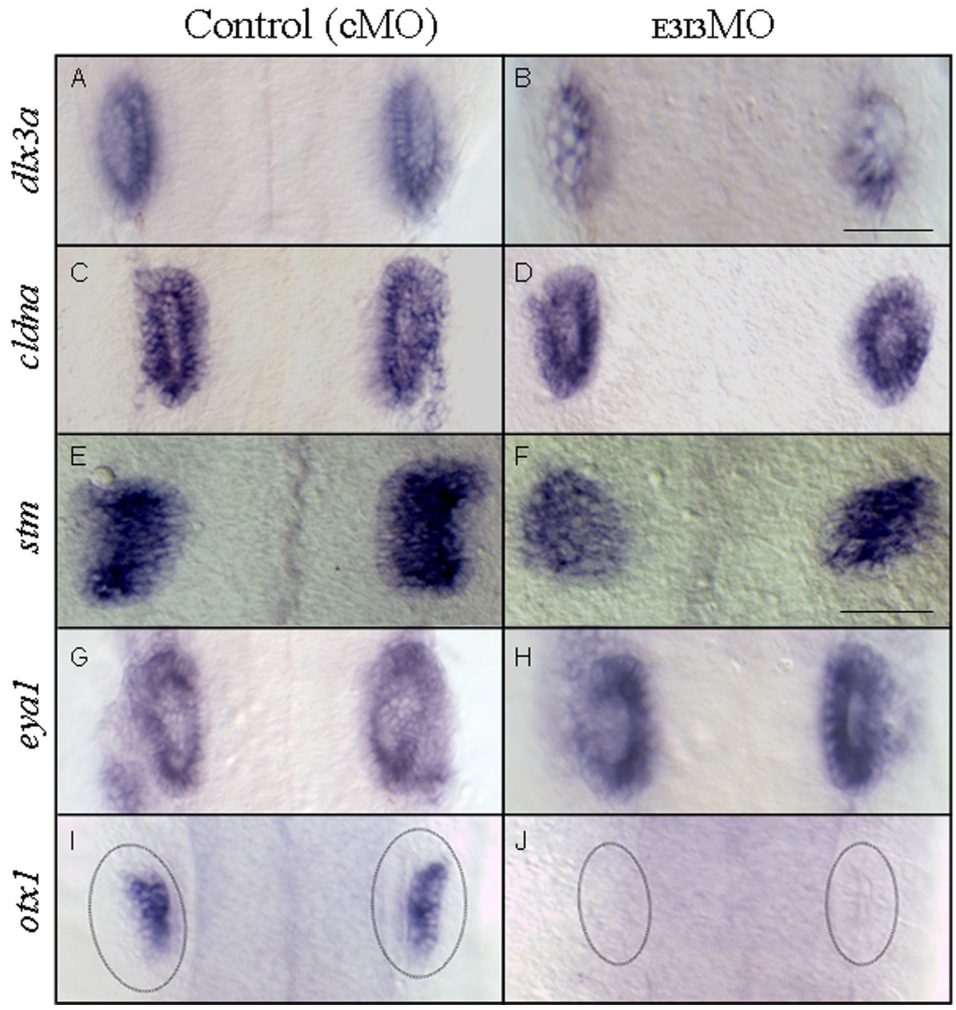

Figure 6. Knockdown of Sparc does not affect otic induction or initial patterning of the otic vesicle

Otic vesicles of control (A,C,E,G,I) and *sparc* MO injected (B,D,F,H,J) 24 hpf embryos. Whole-mount mRNA in situ hybridization with *dlx3b* (A–B), *cldna* (C–D), *stm* (E–F), *eya1* (G–H) or *otx1* (I,J) antisense probes. Note that *otx1* is not expressed in the *sparc* MO injected fish (J). (A–J) Dorsal views, anterior to the top, 24 hpf. Scale bars: (A–D, G, H–J) 100 μm; (E–F) 100 μm.

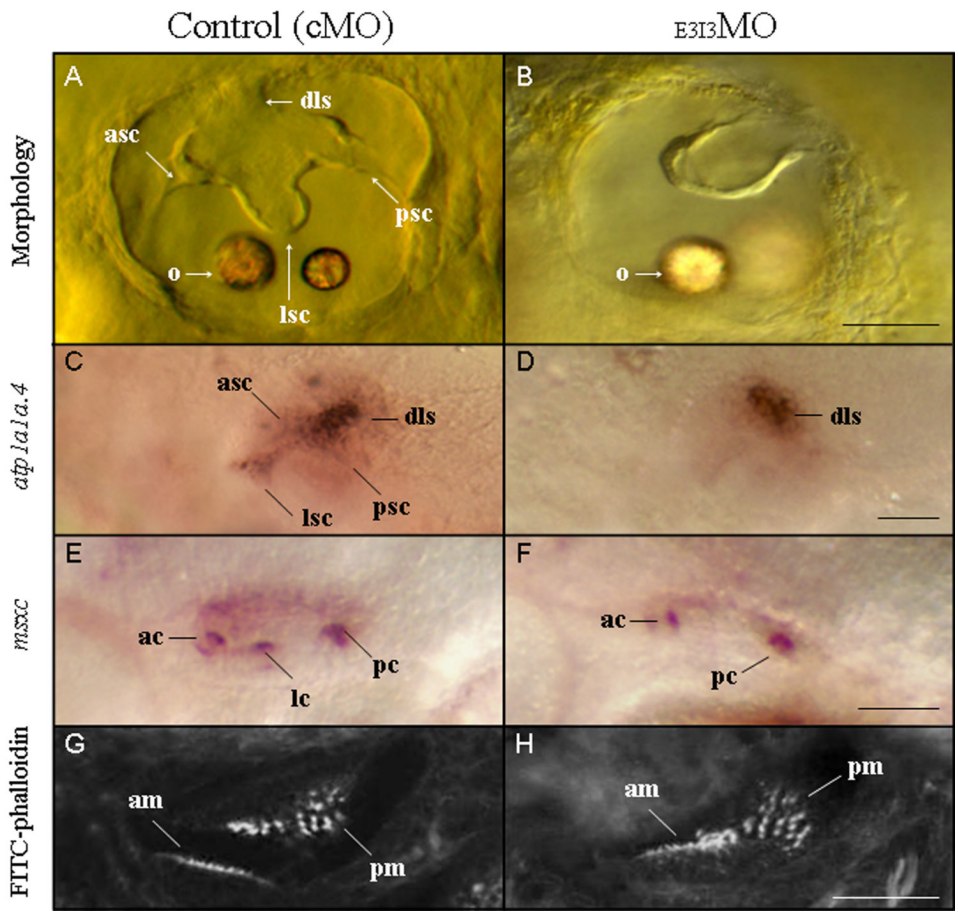

Figure 7. Sparc is required for late morphogenesis of the otic vesicle

Ears of control (A,C,E,G) and *sparc* MO (B,D,F,H) injected animals. (A–B) DIC images of ears of control (A) and *sparc* MO injected embryos (B). In the control, the semicircular canals can be seen. In the MO injected animals, the epithelial projections are formed but fail to elongate or differentiate into semicircular canals. (C–D) mRNA expression of *atp1α1a.4* marks the semicircular canal projections (Blasiole et al., 2003). Note the lack of semicircular canal projections in MO injected embryos (B and D). (E–F) mRNA expression pattern of *msxc* marks the cristae. Note the lack of the lateral crista in MO injected embryos. (G–H) Projections of confocal z-stacks of FITC-phalloidin stained ears reveal the actin-rich stereocilia of the sensory hair bundles. Abbreviations: dls, dorsolateral septum; lc, lateral crista; lsc, lateral semicircular canal projection; psc, posteriror semicircular canal projection; pc, posterior crista; ac, anterior crista; asc, anterior semicircular canal projection; am, anterior macula; pm, posterior macula; o, otholith. (A–H) lateral views, anterior to the left, dorsal to the top; (A–D, G–H) 72 hpf; (E–F) 48 hpf. Scale bars: in B, (A–B) 50 μm; (C–D) 50 μm; (E–F) 50 μm; (G–H) 50 μm.

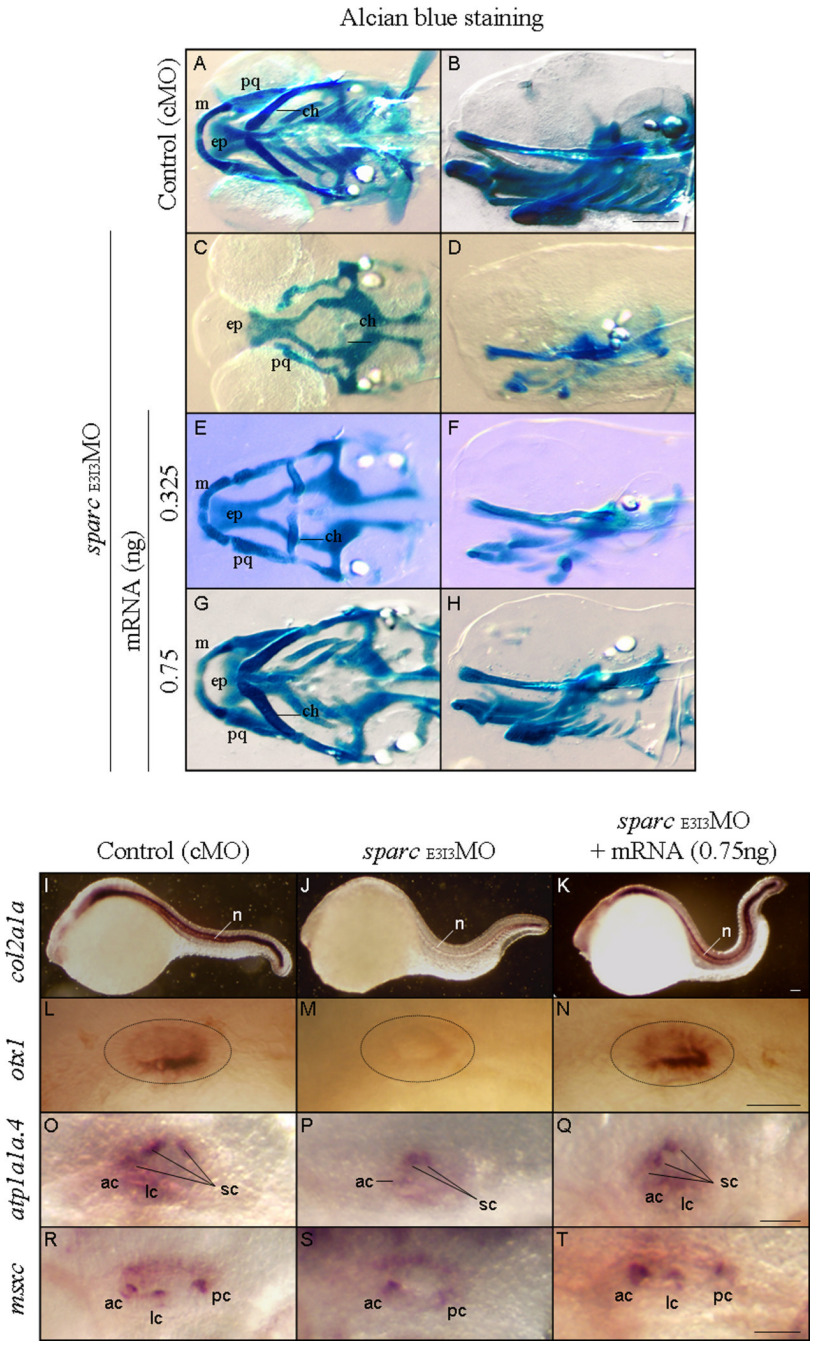

Figure 8. Injection of *sparc* mRNA rescues the phenotype of *sparc* MO-treated embryos

Sense *sparc* mRNA 1 nl of 325 μg/m or 750 μg/ml was coinjected with either 1 nl of 0.5 mM ATG-MO or 1 mM E3I3-MO and the embryos were fixed for in situ hybridization or Alcian blue staining analyses. (A–H) Alcian blue staining reveals cartilage morphology of control (A–B), *sparc* MO injected (C–D), *sparc* MO plus *sparc* mRNA (0.325 ng) (E–F) or *sparc* MO plus *sparc* mRNA (0.75 ng) (G–H) injected animals. (I–T) Whole-mount in situ hybridization analysis of *col2a1* (I–K), *otx1* (L–N), *atp1α1a.4* (O–Q), *msxc* (R–T) expression. (I,L,O,R) Controls, (J,M,P,S) *sparc* MO injected and (K,N,Q,T) *sparc* MO plus *sparc* mRNA (0.75 ng) injected embryos. Abbreviations: ac, anterior crista; lc, lateral crista; pc, posterior crista; sc, semicircular canal projection. (A,C,E,G) ventral views, anterior to the left, 96 hpf. (B,D,F,H)

lateral views, anterior to the left, dorsal to the top, 96 hpf. (I–T) lateral views, anterior to the left, dorsal to the top; (I–N) 24 hpf; (O–T) 48 hpf. Scale bars: (A–H) 100 μm; (I–K) 100 μm; (L–N) 50 μm; (O–Q) 50 μm; (R–T) 50 μm.